waterloopkundig laboratorium
delft hydraulics laboratory

Computation of density currents in estuaries

Extended calibration for inhomogeneous flow in a tidal flume

Report on mathematical investigation

R 897 part VII

Oktober 1980

tow
toegepast onderzoek waterstaat

Computation of density currents in estuaries

Extended calibration for inhomogeneous flow in a tidal flume

Report on mathematical investigation

R 897 part VII

Oktober 1980

tow
toegepast onderzoek waterstaat

CONTENTS

FIGURES

NOTATION

A_0, A_k	Fourier coefficients
a_0	tidal amplitude at sea
B_0, B_k	Fourier coefficients
b	width
C	Chézy coefficient
c	concentration
c_{max}	concentration at sea
$\bar{c}$	depth-averaged concentration
c_g, c_n, c_r	coefficients in the transition function
D_x, D_z	diffusivity in the x- and z-direction respectively
E_D	internal estuary number
F(Ri)	damping function
f(z)	velocity distribution at the upstream boundary
G(Ri)	damping function
g	gravitational acceleration
g(t,z)	transition function
H	depth
HWS	high water slack
L	length
L_f	fictitious length
L_i	intrusion length
LWS	low water slack
l_m	mixing length
MEV	maximal ebb velocity
MFV	maximal flood velocity
N_t	number of time steps
N_x, N_z	number of step sizes in the x- and z-direction respectively
P_t	tidal prism
P	pressure
Q	discharge
Q_r	fresh water discharge
Q_t	tidal discharge
R	hydraulic radius
Ri	local Richardson number
t	time

NOTATION (continued)

T	tidal period
u	velocity in x-direction
u_0	maximal flood velocity
u^*	shear velocity
w	velocity in z-direction
x	longitudinal direction
z	vertical direction
z_b	position of the bottom
z_0	coefficient for roughness length
α	flood number
Δx, Δz	step size, in the x- and z-direction respectively
$\Delta\rho$	density difference between river and sea water
ΔB_0	variation of the mean level
ΔB_1	variation of the amplitude of the vertical tide
$\Delta\phi_1$	variation of the phase of the vertical tide
ΔA_1	variation of the amplitude of the tidal discharge
$\Delta\psi_1$	variation of the phase of the tidal discharge
$\Delta\phi$	variation of the phase difference between upstream and downstream boundary condition
ε_x, ε_z	turbulent diffusion coefficient in the x- and z-direction respectively
κ	Von Karman coefficient
ρ	density
τ	time step
τ_v	time step for momentum equation
τ_D	time step for diffusion equation
ζ	position of the free surface
ζ_0	position of the free surface at x = 0.0 m

COMPUTATION OF DENSITY CURRENTS IN ESTUARIES

Extended calibration for inhomogeneous flow in a tidal flume

1. Introduction

This report is a continuation of [5] in which the calibration of the vertical two-dimensional model for tidal flume circumstances was presented, and in which the term "calibration" was interpreted as the turning of coefficients under the following assumptions:

- the relations in which the coefficients appear describe adequately the phenomena under consideration, and
- the coefficients may vary within a previously fixed range of physically possible values.

In [5] it was also made clear that the calibration presented there was only a limited one, due to the lack of physical insight.
The present report describes an extension of the calibration, including:

- refinements of the numerical methods, and
- further tuning of the coefficients based on extensive examination of available tidal flume measurements [9,7].

The extended calibration leads to some improvement of the correspondence between computations and measurements, but also to the conclusion that there are still systematic differences between the numerical results and the measurements taken from the Delft tidal flume.

In chapter 2 of this report a short review of the measurments is given and in chapter 3 a description of the mathematical model. In chapter 4 some numerical adaptations are described, while in chapter 5 the results of the extended calibration are given.
Finally, conclusions and recommendations are formulated in chapter 6.

This report has been drawn up by Mr. P.A.J. Perrels and is the result of a study which is part of a basic research programme TOW (working group "Stromen en Transportverschijnselen") undertaken by Rijkswaterstaat (Department of Public Works and Water Control), the Delft Hydraulics Laboratory, and other research institutes.

2. Review of the measurements

2.1 Description of the flume

The lucite flume used for the experiments has a rectangular cross-section, 0.67 m wide and 0.50 m high. Two straight sections and the bend between them have a total length of 101.5 m (Figure 1). Downstream the flume discharges into a sea basin, 8 m long, 6 m wide and 1.1 m deeper than the flume, with a control valve generating a periodic tidal movement of the water level. In the test used for the calibration of the 2D-model, the density of the sea water is kept constant by means of a circulation system which pumps salt water into the basin through perforated tubes at the bottom. At the upstream end of the flume there is the equipment necessary to supply separately a constant and a variable discharge of fresh water, thus making it possible to simulate tidal movements which can occur in flumes with a greater length than the actual length (see Figure 1). The variable discharge of fresh water is programmed according to one-dimensional tidal computations for flumes longer than 101.5 m. Fro a detailed description of the flume see Van Rees et al [10].

2.2 Test used for calibration

The results of several tests, with plates (2 x 2 cm) on the bottom of the flume arranged in a diagonal pattern to obtain the desired roughness, are available [6]. For the calibration of the numerical 2D-model in homogeneous tidal circumstances, test T22 was used, while in inhomogeneous tidal circumstances (with density differences) test T20 was chosen. The boundary conditions and flume parameters in these two tests (T22 and T20) are the same, except for the density difference between river and sea water. This difference is zero in test T22 and equal to 23.4 kg m^{-3} in test T20. The following table gives the boundary conditions and the flow paramters of test T20:

quantity	symbol	test T20
depth (averaged over T)	H	0.216 m
fictitious length of flume	L_f	179.34 m
Chézy coefficient	C	19 $m^{\frac{1}{2}} s^{-1}$
tidal period	T	558.75 s
tidal amplitude at sea	a_0	0.025 m
fresh water discharge	Q_r	0.0029 $m^3 s^{-1}$
density difference between river and sea water	$\Delta\rho$	23.4 kg m^{-3}

Table I Boundary conditions and flow parameters

The salinity structure obtained in this test (T20) can be characterized by the following values of the estuary parameters:

the flood number $$\alpha = \frac{Q_r T}{P_t} = 0.39$$

the internal estuary number $$E_D = \frac{u_0^2}{\frac{\Delta\rho}{\rho} g H} \frac{P_t}{Q_r T} = 1.5$$

in which:

P_t: tidal prism, the volume of sea water entering into the flume during the flood period ($\approx 4.5\ m^3$).

u_0: maximum flood velocity at x = 3.66 m (station 1), and

g : gravitational acceleration.

An estuary with these values of the estuary parameters is called partly mixed. At 16 stations at distances n Δx from the mouth of the flume (with n varying from 1 to 16 and Δx = 3.66 m), the water level was measured. In each station the velocities and concentrations were measured at 12 positions in the vertical (with distances $\Delta z = \frac{1}{13} H$ between each other).

The accuracy of the velocities is of the order [6]:

$\sigma_u = 0.0075 \text{ m s}^{-1}$.

The accuracy of the densities is of the order [6]:

$\sigma_\rho = 0.25 \text{ kg m}^{-3}$.

3. Description of the mathematical model

After integration over the width and with the shallow water approximation, the equations for vertical two-dimensional inhomogeneous currents read [3, 4]:

$$\frac{\partial u}{\partial t} + \frac{1}{b}\frac{\partial}{\partial x}(bu^2) + \frac{\partial (uw)}{\partial z} - \varepsilon_x \frac{\partial^2 u}{\partial x^2} - \frac{\partial}{\partial z}\left(\varepsilon_z \frac{\partial u}{\partial z}\right) = -\frac{1}{\rho}\frac{\partial p}{\partial x} \tag{3.1}$$

$$p = p_s + \rho_o g\,(\zeta - z) + g \int_z^{\zeta} \Delta\rho \; d\theta \tag{3.2}$$

$$\frac{\partial \zeta}{\partial t} + \frac{1}{b}\frac{\partial}{\partial x}\left\{b \int_{z_b}^{\zeta} u \; dz\right\} = 0 \tag{3.3}$$

$$\frac{1}{b}\frac{\partial (bu)}{\partial x} + \frac{\partial w}{\partial z} = 0 \tag{3.4}$$

$$\frac{\partial c}{\partial t} + \frac{1}{b}\frac{\partial (buc)}{\partial x} + \frac{\partial (wc)}{\partial z} - \frac{\partial}{\partial x}\left(D_x \frac{\partial c}{\partial x}\right) - \frac{\partial}{\partial z}\left(D_z \frac{\partial c}{\partial z}\right) = 0 \tag{3.5}$$

For ε_z and D_z a mixing length approach is used:

$$\varepsilon_z = l_m^{\,2} \left|\frac{\partial u}{\partial z}\right| F(Ri) \tag{3.6a}$$

$$D_z = l_m^{\,2} \left|\frac{\partial u}{\partial z}\right| G(Ri) \tag{3.6b}$$

in which the mixing length lm is defined by:

$$l_m = \kappa(z + z_0) \qquad 0 \leq z \leq \frac{H}{4}$$

$$l_m = \kappa\left(\frac{H}{4} + z_0\right) \qquad \frac{H}{4} \leq z \leq H.$$

Here z_0 is a measure for the roughness length. F(Ri) and G(Ri) are damping functions, which denote the influence of the stratification on the turbulent exchange of respectively momentum and mass.

An extended derivation of the equations can be found in [2, 8].

The boundary conditions are:

At the bottom, $z = z_b$: $u = 0$ (3.7a)

$w = 0$ (3.7b)

$$D_x \frac{\partial c}{\partial x} \frac{\partial z_b}{\partial x} - D_z \frac{\partial c}{\partial z} = 0 \quad (3.7c)$$

(transport through the bottom is zero)

at the surface, $z = \zeta$: $\frac{\partial u}{\partial n} = 0$ (3.8a)

(no wind influence)

$$D_x \frac{\partial c}{\partial x} \frac{\partial \zeta}{\partial x} - D_z \frac{\partial c}{\partial z} = 0 \quad (3.8b)$$

(transport through the surface is zero)

at the upstream end, $x = L$: $u = f(z)\, Q(t)$ (3.9a)

$c = 0$ (3.9b)

at the downstream end, $x = 0$: $\frac{\partial^2 u}{\partial x^2} = 0$ (3.10a)

$$c = c_{max}\, g(t,z), \text{ if } u > 0 \quad (3.10b)$$

$$\frac{\partial^2 c}{\partial x^2} = 0, \text{ if } u < 0 \quad (3.10c)$$

$$\zeta = \zeta_0(t) \quad (3.10d)$$

4. Numerical modifications

4.1 Review of the modifications

In the first place the discretisation of the boundary conditions for the diffusion equation was changed at the bottom and at the free surface, thus preventing unnecessary extrapolation of concentrations near the boundary.

In the second place, the influence of the discretisation of the Richardson number on the vertical velocity and density distribution was investigated. Several methods appeared to give locally unstable results and measures had to be taken to avoid these instabilities.

A review of the computations and the values of the coefficients used is given in Table II.

The influence of the numerical modifications on the results is shown in:
- Table III, which presents the Fourier components of the tidal elevation, and
- Table IV, which presents the Richardson numbers for several discretisations.

To quantify the influence of any variation in [5], a norm was defined. For the tidal motion this norm was defined as the order of the differences which occur due to a variation of 5% in the Chézy coefficient C, and for the concentration distribution the tolerance of the measurements in the flume was taken as the norm.
The norm reads:

$$\begin{aligned} \Delta B_0 &= 0.0003 \text{ m} \\ \Delta B_1 &= 0.0007 \text{ m} \\ \Delta \phi_1 &= 0.093 \text{ rad} \\ \Delta A_1 &= 0.0005 \text{ m}^3 \text{ s}^{-1} \\ \Delta \psi_1 &= 0.031 \text{ rad} \\ \Delta \rho &= 0.75 \text{ kg m}^{-3} \\ \Delta L_i &= 0.5 \text{ m} \end{aligned} \qquad (4.1)$$

All variations in the results presented in the present report will be considered with respect to this norm.

4.2 Discretisation of the boundary condition for the diffusion equation, at the bottom and the surface

The boundary condition for the diffusion equation reads respectively at the bottom:

$$D_x \frac{\partial c}{\partial x} \frac{\partial z_b}{\partial x} - D_z \frac{\partial c}{\partial z} = 0 \qquad (3.7c)$$

and at the free surface

$$D_x \frac{\partial c}{\partial x} \frac{\partial \zeta}{\partial x} - D_z \frac{\partial c}{\partial z} = 0 \qquad (3.8b)$$

In [3] these relations were discretised directly, thus implying an extrapolation over a layer of thickness Δz, from concentrations in the inner area to the concentration at the boundary, based on (3.7c) or (3.8b).
This is in contradiction with the local meaning of (3.7c) and (3.8b), which are boundary conditions, and so the discretisation was changed. For the present tuning the relations (3.7c) and (3.8b) were substituted into the diffusion equation, which was next discretised. This procedure led to the following difference equations for the computation of the concentration at the bottom respectively at the free surface (see Appendix I):

$$\frac{c^{n+1}_{i,N_z} - c^{n}_{i,N_z}}{\tau} + \frac{(u^{n}_{i+1,N_z} c^{n}_{i+1,N_z} - u^{n}_{i-1,N_z} c^{n}_{i-1,N_z})}{2\Delta x} +$$

$$- \frac{(w^{n}_{i,N_z-1} c^{n+1}_{i,N_z-1} + w^{n}_{i,N_z} c^{n+1}_{i,N_z})}{\Delta z} +$$

$$- \left\{ \frac{D_{x_{i+\frac{1}{2},N_z}} \frac{(c^{n}_{i+1,N_z} - c^{n}_{i,N_z})}{\Delta x} - D_{x_{i-\frac{1}{2},N_z}} \frac{(c^{n}_{i,N_z} - c^{n}_{i-1,N_z})}{\Delta x}}{\Delta x} \right\}$$

$$+ 2 \left\{ \frac{D_{z_{i,N_z-\frac{1}{2}}} \frac{(c^{n+1}_{i,N_z} - c^{n+1}_{i,N_z-1})}{\Delta z}}{\Delta z} \right\} = 0 \qquad (4.2)$$

$$\frac{c_{i,0}^{n+1} - c_{i,0}^{n}}{\tau} + \frac{w_{i,1}^{n} c_{i,1}^{n+1}}{\Delta z} - 2\left\{\frac{D_{z_{i,\frac{1}{2}}} \frac{(c_{i,1}^{n+1} - c_{i,0}^{n+1})}{\Delta z}}{\Delta z}\right\} +$$

$$- \left\{\frac{D_{x_{i+\frac{1}{2},0}} \frac{(c_{1+\frac{1}{2},0}^{n} - c_{i,0}^{n})}{\Delta x} - D_{x_{i-\frac{1}{2},0}} \frac{(c_{i,0}^{n} - c_{i-1,0}^{n})}{\Delta x}}{\Delta x}\right\} = 0 \quad (4.3)$$

The influence of this adaptation is best seen from a comparison of the results of run 4B and 5B.
It appears that the effect is much smaller than the norm (paragraph 4.1), therefore no significant influence of the change in the discretisation of the boundary condition on the calculated results can be observed.

4.3 Discretisation of the Richardson number

In the present model a mixing length approach is used to represent the vertical turbulent exchange [5].
In homogeneous conditions the exchange coefficients read:

$$\varepsilon_z = l_m^2 \left|\frac{\partial u}{\partial z}\right| \quad (4.4)$$

$$D_z = l_m^2 \left|\frac{\partial u}{\partial z}\right|. \quad (4.5)$$

For the present turbulence model, the influence of the stratification is modelled as a function of the Richardson number Ri:

$$R_i = - g \frac{\{\frac{1}{\rho} \frac{\partial \rho}{\partial z}\}}{(\frac{\partial u}{\partial z})^2}. \quad (4.6)$$

The influence of the stratification on the vertical turbulent exchange is given by a set of damping relations. In the present model this set reads [5]:

$$F(Ri) = \exp(-4\,Ri) \quad (4.7)$$

$$G(Ri) = \exp(-15\,Ri). \quad (4.8)$$

(4.7) and (4.8) denote the damping of the vertical turbulent exchange respectively of momentum and mass.
Consequently, the vertical exchange coefficients for respectively momentum and mass read in inhomogeneous conditions:

$$\varepsilon_z = l_m^2 \left|\frac{\partial u}{\partial z}\right| F(Ri) \qquad (4.9)$$

$$D_z = l_m^2 \left|\frac{\partial u}{\partial z}\right| G(Ri) \qquad (4.10)$$

For the discretisation of the Ri-number (4.6) centered differences are used (see Appendix II).
If this discretisation of Ri is substituted directly into the discretised momentum equation wiggles (discontinuities in the gradient) occur in the vertical velocity and concentration distribution (see Figures 2 and 3), especially during falling tide. Quantitatively this numerical behaviour is difficult to predict because of the high degree of non-linearity of the exchange coefficients. This non-linear behaviour is even amplified by the damping functions.
Qualitatively, however, the following explanation can be given:

If locally a stratified situation arises in the concentration, then locally larger Richardson numbers arise. If the opposite situation occurs, locally smaller Richardson numbers arise.
In the first situation the large Richardson number leads to a strong damping of the turbulent exchange, with the result that the stratified situation is maintained. In the opposite case, the smaller Richardson number introduces weaker damping, and the vertically homogeneous situation is maintained. This behaviour is clearly shown in Table IV, run 2B, and in Figures 2 and 3.
As fas as this behaviour is physically relevant, it should be retained. However, numerical amplification should be avoided.

(With respect to Table III, it should be noticed that the results given are after two tidal cycles. Therefore this table cannot be expected to represent periodic conditions, but will merely give tendencies).

Averaging the vertical derivations (see Appendix II) leads to a smoother distribution of the velocity and the concentration (see Table IV, run 3B).

The picture of alternating small and large values in the distribution of Ri has now disappeared, although physically irrelevant values still arise at several locations.

Therefore an extra smoothing of the Ri-numbers was applied (run 4B). In this case, smooth distributions of the velocity, concentration and Ri-numbers arise. However, the physical relevant stratification at $z = \frac{H}{3}$ is retained, (see Table IV).

However, it should be stressed that quantitative comparison of Ri-numbers from computations with those of measurements is severely hampered by the inaccuracies which occur in the calculation of the Ri-numbers.

The influence of averaging on the tidal phenomenon can be seen from Table III. Comparison of the results of the harmonic analysis of 2B with those of 3B shows differences in the free surface elevation which are small compared to the norm (4.1). Summarizing, this differences can be described as:

- an increase of the mean level (1/3 of the norm),
- a decrease of the tidal amplitude (1/4 of the norm, and
- a reduction of the intrusion length (1/5 of the norm).

Comparison of the results of run 3B with those of 4B, shows the influence of the smoothing procedure.
From Table III it can be seen that smoothing has a damping effect on the tidal phenomena (similar to the effect of averaging):

- the mean level increases (1/2 of the norm);
- the tidal amplitude decreases (1/2 of the norm), and
- the intrusion reduces (3/5 of the norm).

Apparently the smoothing yields extra resistance.
This can also be concluded from the velocity profiles shown in Table IV. Run 4B shows velocities which are larger near the bottom and smaller near the surface than those from 3B. Therefore the bottom stress in 4B must be smaller, but the internal stress larger. Finally, this leads to a larger resistance.

4.4 New reference situation

When the numerical modifications were made, a new reference computation was required as a starting-point for the continued tuning, and these were implemented in run III. For the parameters the values from II (the best approximation from [5]) were substituted (see Table II).
Tables V and VI show the variations due to the numerical modifications. When comparing the results of III and II with the measurements it can be seen that, the mean level of the surface decreases (1/3 of the norm), the tidal amplitude increases (1/3 of the norm), there is a small phase shift (1/9 of the norm), and the intrusion increases (about 3 times the norm).

Summarizing the results of II and III it may be concluded that, on the average, the tidal phenomena remain the same. In comparison with the measurements, the salt intrusion improves, although not enough to finish the calibration.

5. The tuning

5.1 Review of the variations

In [5] the damping of the vertical turbulent exchange due to stratification appeared to have a large influence on the results of the computations. Further, the results of [5] were still preliminary, and one of the recommendations was to gather further physical insight into the influence of the stratification on the vertical turbulent exchange.
An extensive examination of the tidal flume measurements [9], from which the relations used in [5]:

$$F(Ri) = \exp(-4\,Ri) \tag{4.7}$$

$$G(Ri) = \exp(-15\,Ri) \tag{4.8}$$

were taken, showed that, especially for the influence on the vertical exchange of salt content, even a stronger damping was physically possible (see Figure 4). Moreover, from the sensitivity analysis, reported in [5], it should be concluded that a stronger damping of the vertical mass exchange would yield a better correspondence between computations and measurements.
The damping of the vertical momentum exchange (4.7) has, however, been unchanged to preserve the existing correspondence between computed and measured tidal motion.
Therefore, it was decided to make a computation with the following damping functions:

$$F(Ri) = \exp(-4\,Ri) \tag{5.1}$$

$$G(Ri) = \exp(-18\,Ri) \tag{5.2}$$

Besides the damping functions also the salt concentration of the sea water was changed and raised from 22.8 kg m^{-3} to 23.4 kg m^{-3}.

From the sensitivity analysis in [5] also the influence of the longitudinal dispersion on the intrusion length became clear. Therefore next to the tuning of the turbulent exchange coefficients, the coefficient a in the dispersion relation:

$$D_x = a\,|u^*|\,b, \qquad (5.3)$$

was tuned.

In computation IV (see Table II), this coefficient was taken equal to 3, while in V it was raised to 4.5.

5.2 Tuning of the vertical turbulent exchange coefficients

Comparison of the harmonic analysis of the free surface elevations and the discharges of the computions III, IV (see Table II) with those of the measurements (T20) shows (see Table V):

- that at x = 3.66 the amplitude of the tidal discharge of IV has become slightly worse than that of III (about 1/5 of the norm (4.1));
- that at x = 3.66 m the phase of the tidal discharge of IV is slightly better then that of III (about 1/4 of the norm) and at x = 47.58 slightly worse than that of III (about 1/4 of the norm);
- that downstream the mean water level of IV is slightly better (about 1/2 of the norm) than that of III;
- that on the average the amplitude of the free surface elevation remains the same; and
- that in IV the phase of the free surface elevation slightly improves (about 1/9 of the norm) compared to III.

Summarizing, it can be said that the tidal movement slightly improves.

To compare the results for the salt distribution, three aspects are distinguished:

- the stratification,
- the intrusion, and
- the longitudinal distribution.

When comparing the results of IV and III, the stratification becomes stronger throughout the tidal cycle. Compared with the measurements (see Figure 5) the order of the stratification is just about right around MEV and MFV.
Around HWS it is too weak, especially near the surface, and around LWS the stratification is too strong.

From Table VI and from Figures 5 and 6 it can be concluded that the intrusion increases throughout the tidal cycle except around HWS. This implies that the maximal intrusion is unchanged. Comparison with the measurements shows that the maximal intrusion is still too small.

From Table VI it can be seen that the longitudinal distribution has changed too. At HWS the position of the 1 kg-isopycnyc is unchanged, but the positions of the 5 kg- and 20 kg-isopycnyc have changed, respectively 0.3 m and 0.8 m in upstream direction.
Comparison of the intrusion lengths at HWS and LWS shows that the difference between minimal and maximal intrusion has decreased with 3 m to 8 m respectively for the 1 kg- and the 20 kg-isopycnyc.

Comparison of the intrusion length from the measurements with the computed ones still shows significant differences, especially for the distance between the 1 kg- and the 5 kg-isopycnyc.
In the measurements the longitudinal gradient near the top of the salt wedge is much larger than in the computations.

5.3 Tuning of the longitudinal dispersion coefficient

As can be seen from Table V, the influence of the variation of the dispersion coefficient on the tidal phenomena is small: the differences between run IV and V are about 1/5 of the order of the norm (4.1), or less.

This behaviour corresponds well with the results of the aforementioned sensitivity analysis [5].

The influence of the enlargement of the dispersion coefficients on the salt distribution can be seen from Figures 7 and 8 and from Table VI.
The following aspects of the salt distribution are distinguished:
- the stratification
- the intrusion
- the longitudinal distribution.

When comparing the results of runs IV and V it appears that the stratification has hardly changed. This implies that considering the stratification in run V the same phenomena occur as in run IV, reported in 5.2.

With respect to the intrusion, it can be concluded that the maximal intrusion increases throughout the whole tidal cycle.
This can be seen from the position of the 1 kg-isopycnyc in Figure 7, as well as from the maxima of the depth-averaged concentrations shown in Figure 8. Moreover, it can also be seen from Table VI.

Comparison of the maximal intrusion lengths of run V with the measured ones shows a good correspondence during the whole tidal cycle. Except around LWS, when the difference is about twice the norm, the differences are within the norm.

For the longitudinal distribution of runs IV and V the conclusion is that in V the longitudinal spreading of salt has increased compared to IV. From Figure 7 and Table VI it is readily seen that the intrusion of the 20 kg-isopycnyc has decreased, and although the intrusion of the 5 kg-isopycnyc has increased, it is much less than that of the 1 kg-isopycnyc.

When the results of V are compared with the measurements, it appears that the longitudinal distribution has become worse than it was in IV.

When the longitudinal density gradient from computation V is plotted against the measured one, the following tendency can be seen:

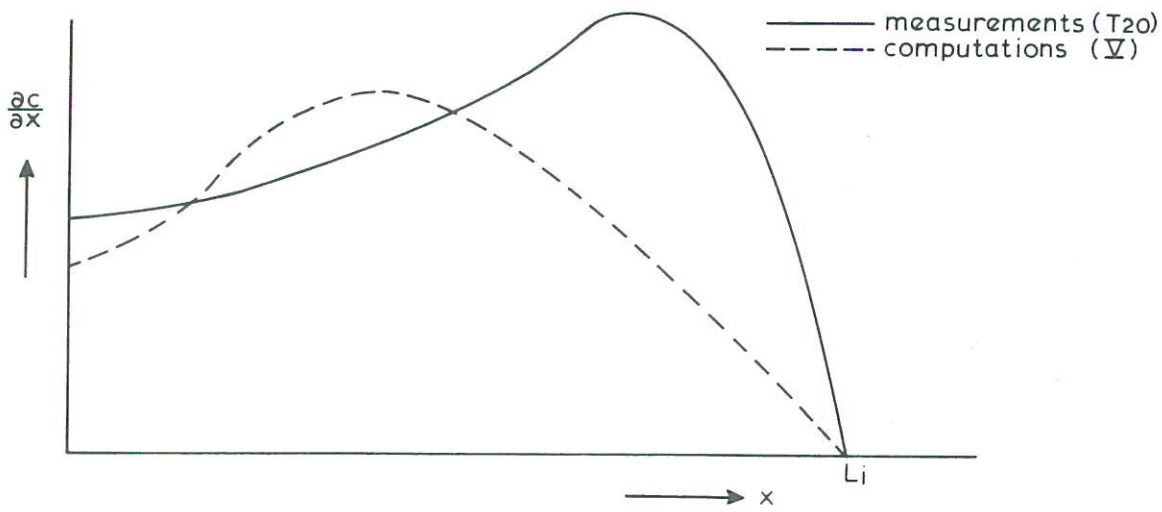

The gradients from the computation have a more gradual course than those from the measurements.

In [7] an estimation of the 2D-dispersion coefficient is given. From that result, it follows that the values of $D_x/|u^*|b$ in equation (5.3) used in the present 2D-computations are too large.

5.4 Conclusions of the tuning

From the results of the tuning, the following conclusions can be drawn:

- the results of the numerical model have improved. In the first place with respect to the maximal intrusion, but also considering the stratification and for a minor part the tidal phenomena.
- the tidal phenomena have been well calibrated.
- the overall picture of the salt intrusion is satisfactory.

However, when going into details:

- There are still systematic differences between the computed and the measured results, especially concerning the longitudinal salt distribution. There also differences in the stratification.
  The differences in the tidal phenomena between measurements and computations, at x = 10.98 m and x = 18.3 m probably correspond to the differences in the concentration.
- With the present relations for the longitudinal dispersion and the vertical turbulent transport no further improvement of the results can be expected.

Indications for a possible limitation of the present relations is given in [1], where it is argued that the choise of the length scale of turbulence (the mixing length of equations (3.6a) and (3.6b)) possibly should reflect that estuarine turbulence can be generated both externally (at the solid bottom) and internally (because of density effects).

6. Conclusions and recommendations

6.1 Conclusions

In the present report the calibration for tidal flume circumstances has been extended with a further tuning of:

- the coefficients for the vertical turbulent exchange, and
- the longitudinal dispersion coefficient.

Considering the coefficient for the vertical turbulent exchange, two aspects are of interest:

a the form of the damping relations F(Ri) and G(Ri).
From the final results it can be concluded that the present model still shows systematic differences from the tidal flume phenomena.
The mean differences consist in:
- a different longitudinal density distribution, and
- a different behaviour of the stratification.

From the results of the present report and those of [5], it is concluded that these differences are chiefly due to the formulation of the vertical turbulent exchange.

b the discretisation of the Ri-number.
From the several computation it appeared that not-to-careful discretisation of Ri leads to locally unstable results. These instabilities were suppressed by averaging and smoothing.

A test on the correctness of the computed Ri-numbers by comparison with those from measurements is impossible, as long as Ri-numbers cannot be accurately calculated.

With regard to the longitudinal dispersion coefficient, the tuning has provided the correct order of magnitude in the sense that the computed maximal intrusion corresponds well with the measured one.
However, the values of the dispersion coefficients are too large in comparison with those taken from measurements [7].

6.2 Recommendations

Further investigation with regard to the tidal flume calibration should be concentrated in the first place on understanding from a physical point of view the influence of the stratification on the vertical turbulent exchange. In the present model this influence is modelled as a set of damping functions, which depend on the Ri-number.

In [1] it is argued that the choice of the length scale of turbulence (mixing length of (3.6a) and (3.6b)) does not reflect that estuarine turbulence can be generated both externally (at the solid bottom) and internally (because of density effects).
The consequence is that turbulence generated externally and internally should be modelled separately, with different length scales.
If the concept of one length scale is retained, the damping functions used in (3.6a) and 3.6b) should vary with the stage of the tide, as suggested in [1].
This length scale probably will not be a function of the distance to the bottom. Therefore a locally determined length scale, as suggested by Von Karman, may be preferable. From the point of predictive capabilities, a multi-scale approach is preferable.
A more definite indication at this point could come from a comparison of the present mixing length model with a more sophisticated turbulence model, provided it describes the effect of buoyancy on the vertical turbulent exchange correctly. As a first step the order of magnitude, of terms which are neglected when using a mixing length approach, could be investigated for tidal flume circumstances. If they turn out to be small this provides a justification of the mixing length model under these circumstances. In the opposite case this may give indications for possible extensions of the turbulence model.
A second important indication might come from measurements whose accuracy should permit the computation of damping functions and Ri-numbers throughout a tidal cycle.
Moreover, accurately calculated Ri-numbers from measurements would permit a comparison with Ri-numbers from computations. And this could give indications for the optimal discretisation of the Ri-numbers.

REFERENCES

1 ABRAHAM, G.
On internally generated estuarine turbulence,
Paper presented at Sec. Int. Symp. on stratified flows, Trondheim, 1980.

2 Delft Hydraulics Laboratory,
Computational methods for the vertical distribution of flow in shallow water.
Report on literature study, W 152, 1973.

3 Delft Hydraulics Laboratory,
Computation of density currents in estuaries, the homogeneous model.
Report on mathematical investigations, R 897-III, December 1976, in Dutch.

4 Delft Hydraulics Laboratory,
Computation of density currents in estuaries, numerical accuracy of the model.
Report on mathematical investigations, R 897-IV, June 1979.

5 Delft Hydraulics Laboratory,
Computation of density currents in estuaries, calibration for inhomogeneous flow in a tidal flume.
Report on mathematical investigations, R 897-VI, February 1980.

6 Delft Hydraulics Laboratory,
Investigation with bottom roughness for the verification of a two-dimensional numerical salt intrusion model.
Report on model investigations, M 897-38B, March 1980, in Dutch.

7 Delft Hydraulics Laboratory,
The influence of lateral variations on the diffusive transport.
To be published (in Dutch), report M 896-46, 1980.

8 PERRELS, P.A.J. and KARELSE, M.
A two dimensional numerical model for salt intrusion in estuaries.
Delft Hydraulics Laboratory, publication 177, 1977.

REFERENCES (continued)

9 REES, A.J. van
Experimental results on exchange coefficients for non-homogeneous flow.
XVIthe IAHR Congress, Paper C 36, 1975.

10 REES, A.J. van and RIGTER, B.P.
Flume study on salinity intrusion in estuaries.
XIIIth IAHR Congress, Paper C 33, 1969.

parameter number of the calculation	L m	H m	T s	Q_r $m^3 s^{-1}$	ε_x $m^2 s^{-1}$	D_x [1] $m^2 s^{-1}$	N_x	N_z	N_t	τ_v s	τ_D s	$\Delta\rho$ kg m^{-3}	c_g [2] kg m^{-3} s^{-1}	F(Ri) [3]	G(Ri) [3]	Bc [4] z=0,H	R_i [5]	C [6] $m^{\frac{1}{2}} s^{-1}$	CPU [7] 3
2B	100.65	.216	558.75	.0029	.37	a	55	24	1200	.93	.23	22.8	α	DTF 1	DTF 1	E	L2	first 61.3 m/last 39.35 m 21.6 / 19.6	752
3B	100.65	.216	558.75	.0029	.37	a	55	24	1200	.93	.23	22.8	α	DTF 1	DTF 1	E	ML2	21.6 / 19.6	772
4B	100.65	.216	558.75	.0029	.37	a	55	24	1200	.93	.23	22.8	α	DTF 1	DTF 1	E	SL2	21.6 / 19.6	744
5B	100.65	.216	558.75	.0029	.37	b	55	24	1200	.93	.23	23.4	α	DTF 2	DTF 2	R	SL2	21.6 / 19.6	788
II	100.65	.216	558.75	.0029	.37	a	55	24	4800	.93	.23	22.8	α	DTF 1	DTF 1	E	L1	21.6 / 19.6	3514
III [8]	100.65	.216	558.75	.0029	.37	a	55	24	4800	.93	.23	22.8	α	DTF 1	DTF 1	E	L2	21.6 / 19.6	3388
IV	100.65	.216	558.75	.0029	.37	a	55	24	4800	.93	.23	23.4	α	DTF 2	DTF 2	R	SL2	21.6 / 19.6	3494
V	100.65	.216	558.75	.0029	.37	b	55	24	4800	.93	.23	23.4	α	DTF 2	DTF 2	R	SL2	21.6 / 19.6	3450

1) the letters denote: a - 3.0 $|u^*|$b + 0.15
b - 4.5 $|u^*|$b + 0.15

2) the greek letter denote: $\alpha = c_n + 3 \frac{(H-z)}{H} c_n$

3) DTF 1: F(Ri) = exp (- 4 Ri) G(Ri) = exp (-15 Ri)
DTF 2: F(Ri) = exp (- 4 Ri) G(Ri) = exp (-18 Ri)

4) E: boundary condition inposed by extrapolation
R: boundary condition substituted; yields reduced diffusion equation

5) L1 : Ri computed at level $j\Delta z$; ε_z and D_z middled
L2 : Ri computed at level $(j+\frac{1}{2})\Delta z$
ML_2 : Ri computed at level $(j+\frac{1}{2})\Delta z$; $(\frac{\partial u}{\partial z})$ and $(\frac{\partial \rho}{\partial z})$ middled
SL_2 : Ri computed at level $(j+\frac{1}{2})\Delta z$; $(\frac{\partial u}{\partial z})$ and $(\frac{\partial \rho}{\partial z})$ middled; Ri smoothed

6) in a steady state C is related to z_0 by: $C = 18 \log \frac{12 R}{33 z_0}$, in which R is the hydraulic radius.

7) on a CDC-6600 computer

8) new reference situation (see Paragraph 4.4).

Table II List of the calculations with the values of the parameters

position	quantity	2B	3B	4B	5B
3.66 m	A_o (m^3s^{-1})	- .0029	- .0029	- .0029	- .0029
	A_1 (m^3s^{-1})	.0287	.0287	.0287	.0287
	ψ_1 (rad)	- 1.996	- 1.995	- 1.996	- 1.996
	B_o (m)	.2162	.2163	.2163	.2164
	B_1 (m)	.0239	.0237	.0237	.0237
	ϕ_1 (rad)	1.647	1.647	1.647	1.646
10.98 m	B_o	.2167	.2169	.2170	.2169
	B_1	.0234	.0232	.0231	.0231
	ϕ_1	1.759	1.759	1.759	1.759
18.30 m	B_o	.2173	.2174	.2175	.2175
	B_1	.0232	.0230	.0227	.0229
	ϕ_1	1.862	1.864	1.865	1.865
25.62 m	B_o	.2180	.2181	.2183	.2182
	B_1	.0231	.0230	.0226	.0229
	ϕ_1	1.973	1.972	1.979	1.974
32.94 m	B_o	.2188	.2189	.2191	.2190
	B_1	.0230	.0229	.0225	.0228
	ϕ_1	2.096	2.096	2.104	2.095
40.26 m	B_o	.2195	.2196	.2197	.2196
	B_1	.0229	.0228	.0225	.0227
	ϕ_1	2.216	2.216	2.225	2.216
47.58 m	A_o	- .0029	- .0029	- .0029	- .0029
	A_1	.0237	.0237	.0237	.0237
	ψ_i	- 1.785	- 1.784	- 1.786	- 1.786
	B_o	.2200	.2201	.2202	.2201
	B_1	.0229	.0228	.0225	.0228
	ϕ_1	2.325	2.325	2.334	2.324
	L_i (m)	43.1	43.0	42.7	45.1

Table III Results of the harmonic analysis of the tidal variations in the discharge and the water level (after two tidal cycles)

run number	2B			3B			5B			4B		
position (Z/H)	velocity ms^{-1}	concentration kgm^{-3}	Ri-number	velocity ms^{-1}	concentration kgm^{-3}	Ri-number	velocity ms^{-1}	concentration kgm^{-3}	Ri-number	velocity ms^{-1}	concentration kgm^{-3}	Ri-number
1.0000	.332	.498	.00*	327	.519	.64	.309	.938	2.19	.303	.463	1.69
.9584	.332	.497	.41	.327	.519	.66	.309	.994	1.43	.303	.552	1.57
.9167	.324	.799	.00*	.319	.750	1.56	.305	1.167	.88	.299	.698	1.25
.8750	.323	.799	.14	.317	.896	3.41	.300	1.343	.76	.297	.805	.96
.8333	.313	.954	.00*	.316	1.009	.46	.296	1.527	.72	.293	.939	.81
.7916	.313	.954	.47	.312	1.255	.20	.291	1.702	.70	.289	1.085	.74
.7500	.305	1.293	.09*	.294	1.533	.44	.286	1.882	.74	.285	1.226	.68
.7084	.304	1.294	.09	.293	1.631	6.26	.281	2.118	.75	.280	1.408	.63
.6667	.284	1.714	.09*	.292	1.660	.44	.275	2.413	.71	.274	1.674	.64
.6250	.283	1.715	.67	.287	2.640	.13	.269	2.723	.69	.268	1.898	.65
.5833	.270	2.898	.17*	.254	3.055	.20	.262	3.054	.69	.262	2.125	.63
.5416	.268	2.903	.17	.253	3.176	6.97	.255	3.498	.72	.255	2.508	.63
.5000	.227	4.805	.17*	.251	3.243	.39	.247	3.936	.78	.247	2.903	.71
.4584	.224	4.822	.61	.246	4.966	.07	.239	4.525	.89	.238	3.504	.84
.4167	.207	6.834	.02	.199	5.125	.04	.229	5.528	.72	.225	4.898	.86
.3750	.203	6.830	.14	.198	5.131	6.78	.215	7.015	.42	.210	7.325	.49
.3333	.159	9.872	.01	.194	5.238	.64	.206	9.140	.21	.202	9.330	.28
.2916	.156	9.873	.03	.182	12.703	.14	.150	10.008	.68	.146	10.214	.97
.2500	.147	9.905	0.01	.117	12.932	.02	.146	12.848	1.07	.140	12.907	1.57
.2084	.124	9.955	3.94	.114	12.968	.26	.140	13.021	.59	.136	13.004	.78
.1667	.112	16.472	.00	.110	13.009	.20	.135	13.136	.13	.131	13.055	.05
.1250	.082	16.499	.01	.091	13.593	.09	.096	14.521	.04	.093	13.592	.03
.0833	.068	16.530	.01	.071	13.902	.02	.070	15.224	.04	.073	13.795	.02
.0416	.047	16.566	.01	.048	14.001	.01	.046	15.461	.02	.050	13.923	.01
.0000	.000	16.599		.000	14.059		.000	15.543		.000	14.004	

* inaccurate Richardson number

Table IV Review of the velocities, concentration and Ri-numbers at x = 18.3 m and t = 0.68 T

position	quantity	T20	III	IV	V	II
3.66 m	A_o (m^3s^{-1})	- .0029	- .0029	- .0029	- .0029	- .0029
	A_1 (m^3s^{-1})	.0271	.0289	.0290	.0289	.0289
	ψ_1 (rad)	1.084	1.134	1.126	1.126	1.140
	B_o (m)	.2163	.2163	.2163	.2164	.2163
	B_1 (m)	.0235	.0237	.0237	.0237	.0237
	ϕ_1 (rad)	- 1.665	- 1.650	- 1.648	- 1.648	- 1.648
10.98 m	B_o	.2176	.2168	.2169	.2169	.2169
	B_1	.0229	.0232	.0230	.0230	.0230
	ϕ_1	- 1.812	- 1.769	- 1.769	- 1.766	- 1.766
18.30 m	B_o	.2180	.2173	.2175	.2175	.2175
	B_1	.0230	.0230	.0229	.0228	.0228
	ϕ_1	- 1.845	- 1.875	- 1.876	- 1.876	1.875
25.62 m	B_o	.2182	.2181	.2181	.2181	.2182
	B_1	.0233	.0229	.0231	.0230	.0227
	ϕ_1	- 1.941	- 1.978	- 1.974	- 1.976	- 1.982
32.94 m	B_o	.2191	.2189	.2189	.2189	.2190
	B_1	.0235	.0230	.0233	.0232	.0228
	ϕ_1	- 2.042	- 2.088	- 2.078	- 2.079	- 2.096
40.26 m	B_o	.2196	.2197	.2197	.2196	.2197
	B_1	.0232	.0232	.0235	.0234	.0229
	ϕ_1	- 2.140	- 2.203	- 2.191	- 2.190	- 2.213
47.58 m	A_o	- .0028	- .0029	- .0029	- .0029	- .0029
	A_1	.0233	.0238	.0238	.0238	.0237
	ψ_1	1.346	1.344	1.336	1.336	1.350
	B_o	.2203	.2202	.2202	.2202	.2203
	B_1	.0234	.0233	.0236	.0235	.0230
	ϕ_1	- 2.250	- 2.310	- 2.296	- 2.295	- 2.321

Table V Results of the harmonic analysis of the tidal variations in the discharge and water level

time	isopycne	T20	III	IV	V	VI
M.T.V.	1- kg	36.0	33.2	34.4	35.8	31.4
	5- kg	35.1	28.1	29.1	29.6	26.6
	20- kg	16.4	15.2	16.1	15.3	14.6
H.W.S.	1- kg	47.1	45.6	45.6	47.0	44.0
	5- kg	42.4	38.6	38.9	39.3	38.1
	20- kg	28.6	25.4	26.2	25.4	24.9
M.E.V.	1- kg	37.4	34.4	35.1	36.9	33.1
	5- kg	35.6	29.1	31.0	31.3	28.0
	20- kg	11.2	11.0	12.8	11.5	9.9
L.W.S.	1- kg	25.5	21.6	23.5	24.6	20.5
	5- kg	25.0	18.7	20.5	20.7	16.7
	20- kg	-	2.9	4.2	3.4	2.8

Table VI Review of the intrusion lengths (m) of several isopycnes

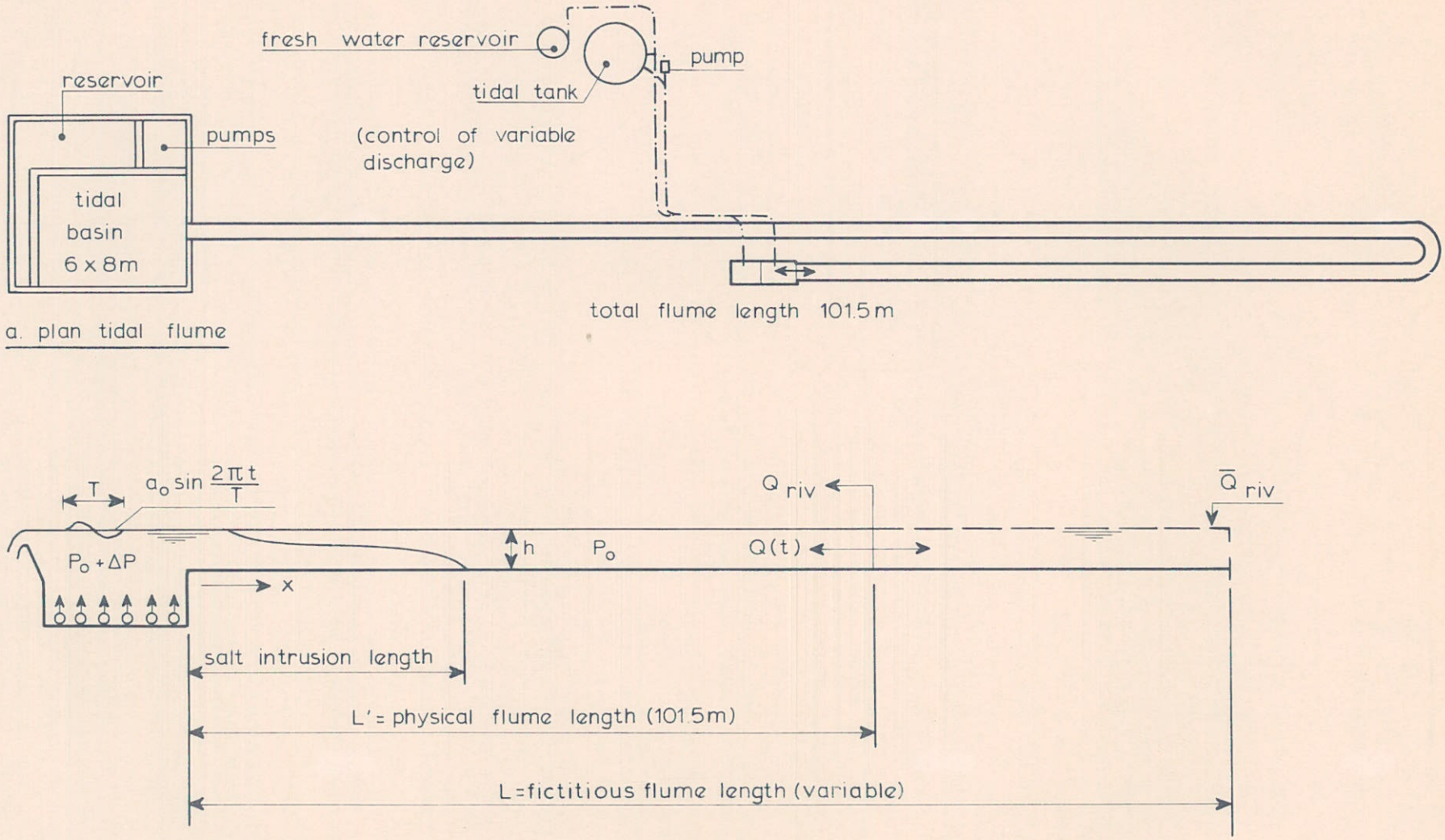

SETUP OF TIDAL SALINITY FLUME WITH NOTATIONS

DELFT HYDRAULICS LABORATORY

R 897-VII

FIG. 1

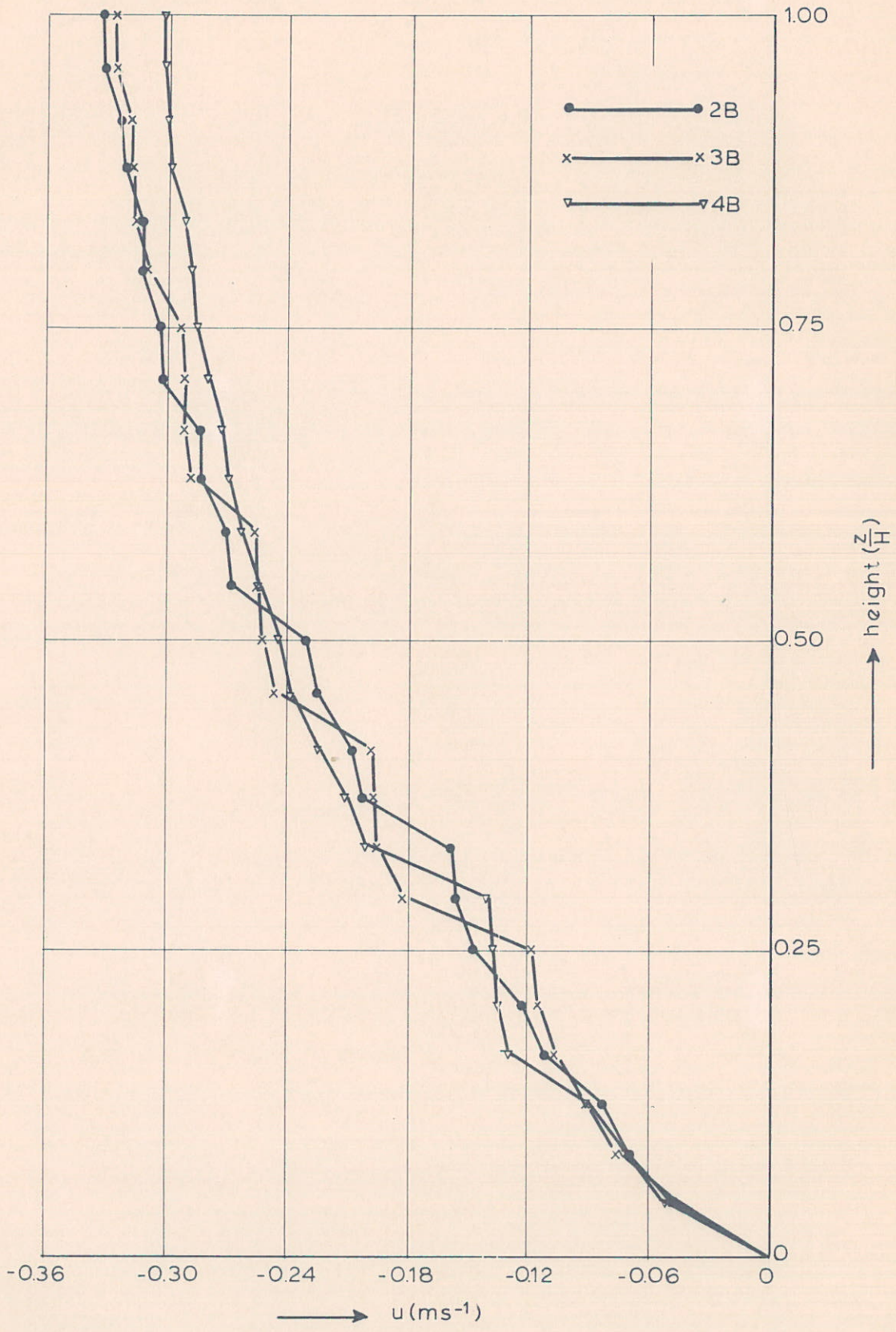

CALIBRATION WITH TIDAL FLUME DATA

VELOCITIES AT x=18.3m AND AT t=0.68T

DELFT HYDRAULICS LABORATORY | R 897 VII | FIG. 2

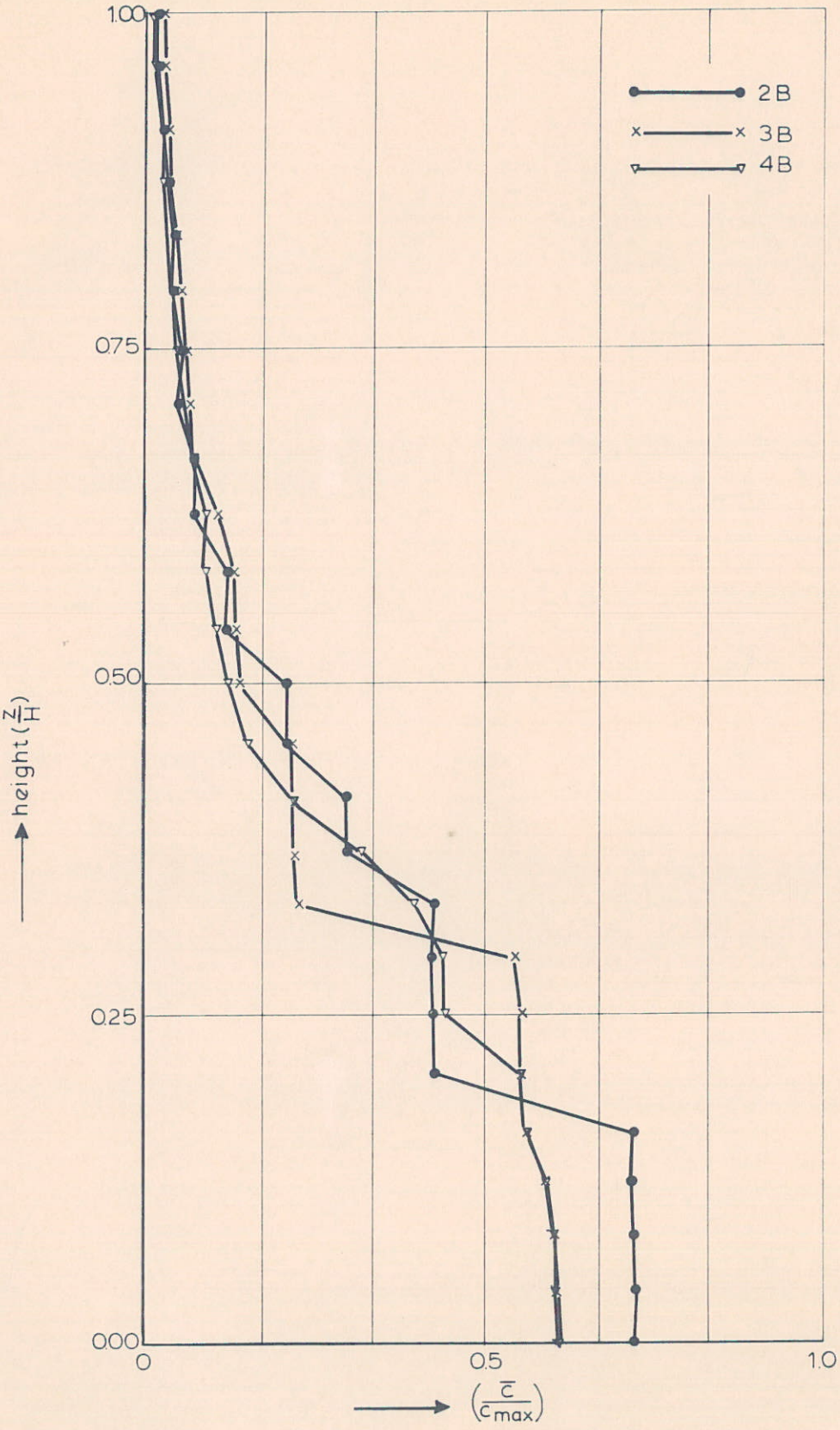

CALIBRATION WITH TIDAL FLUME DATA
CONCENTRATION AT x=18.3m AND AT t=0.68 T

DELFT HYDRAULICS LABORATORY | R 897 VII | FIG. 3

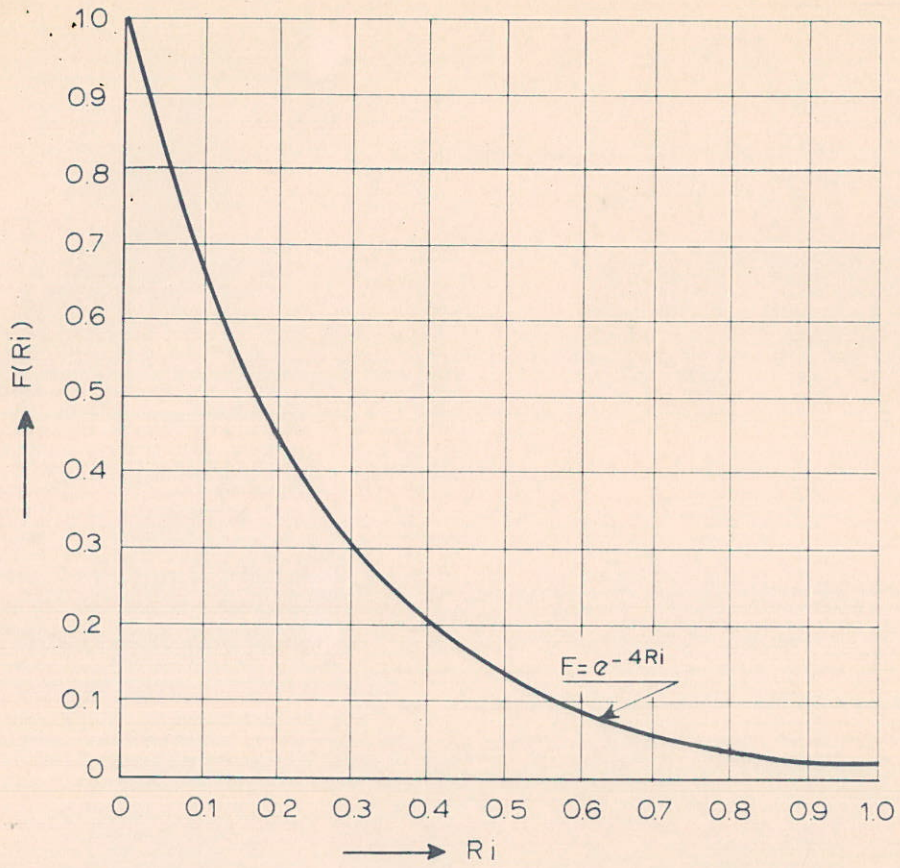

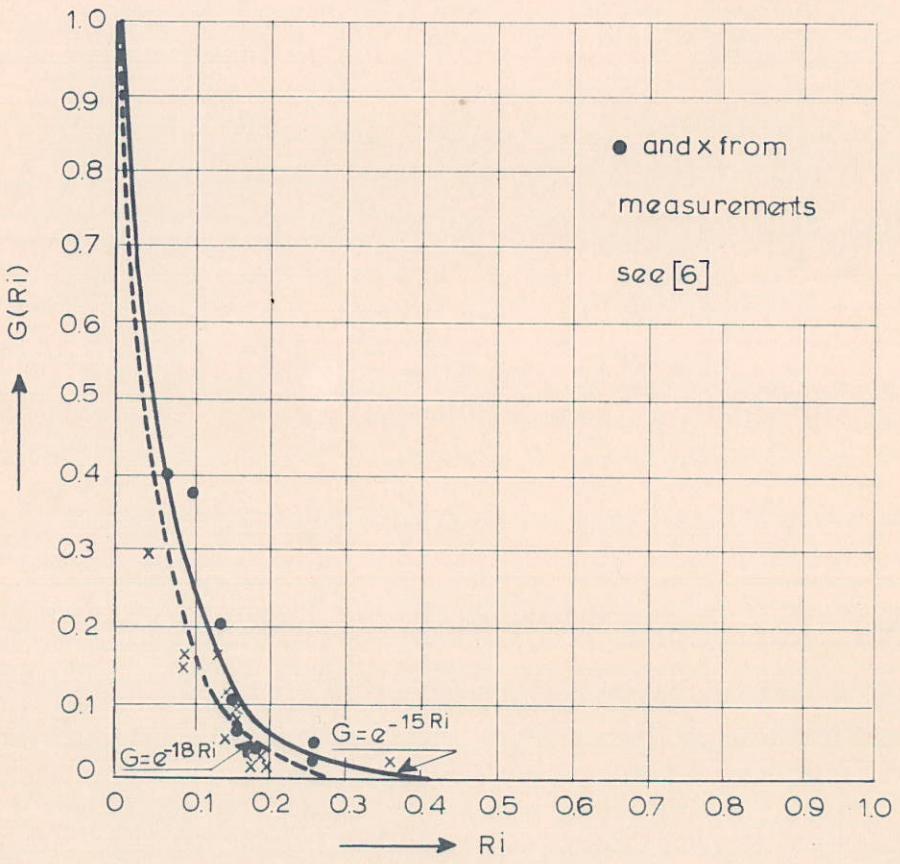

DAMPING FUNCTIONS F(Ri) AND G(Ri)

DELFT HYDRAULICS LABORATORY | R 897 VII | FIG. 4

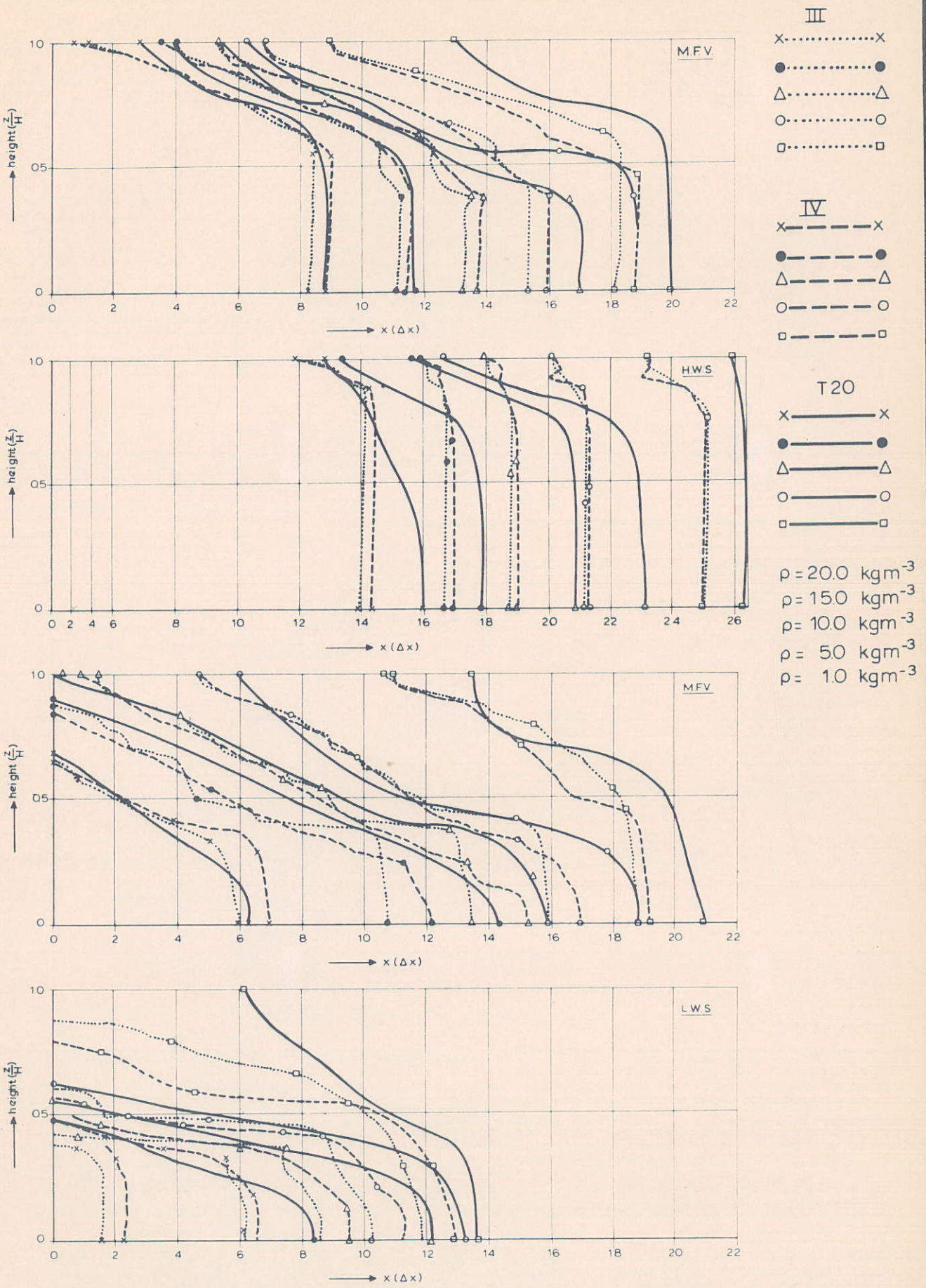

CALIBRATION WITH TIDAL FLUME DATA
LONGITUDINAL CONCENTRATION DISTRIBUTION
AT FOUR CHARACTERISTIC TIMES

Δx=1.83m

DELFT HYDRAULICS LABORATORY

R 897 VII

FIG. 5

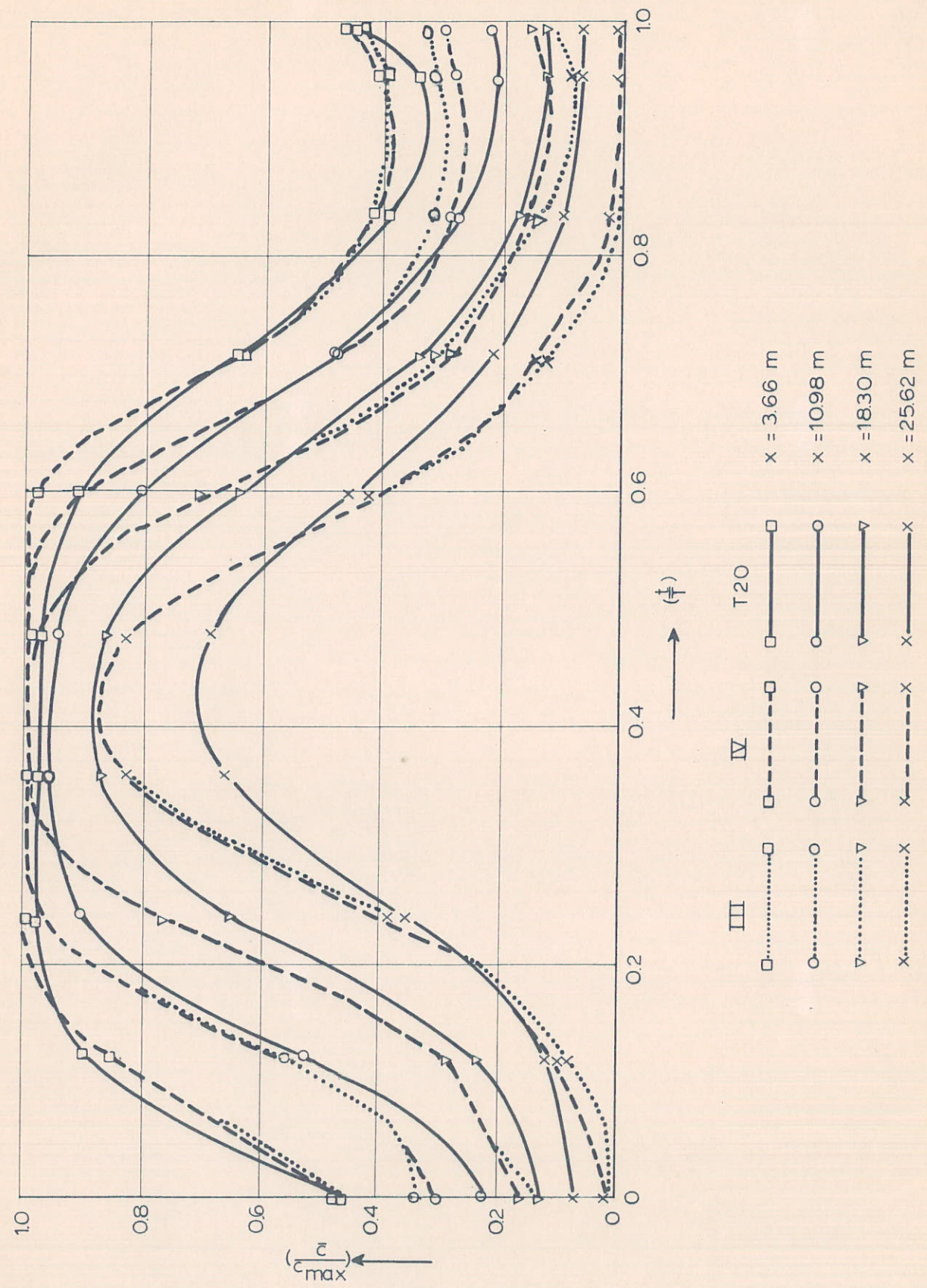

CALIBRATION WITH TIDAL FLUMEDATA
RELATIVE DEPTH AVERAGED CONCENTRATIONS

DELFT HYDRAULICS LABORATORY | R 897 VII | FIG. 6

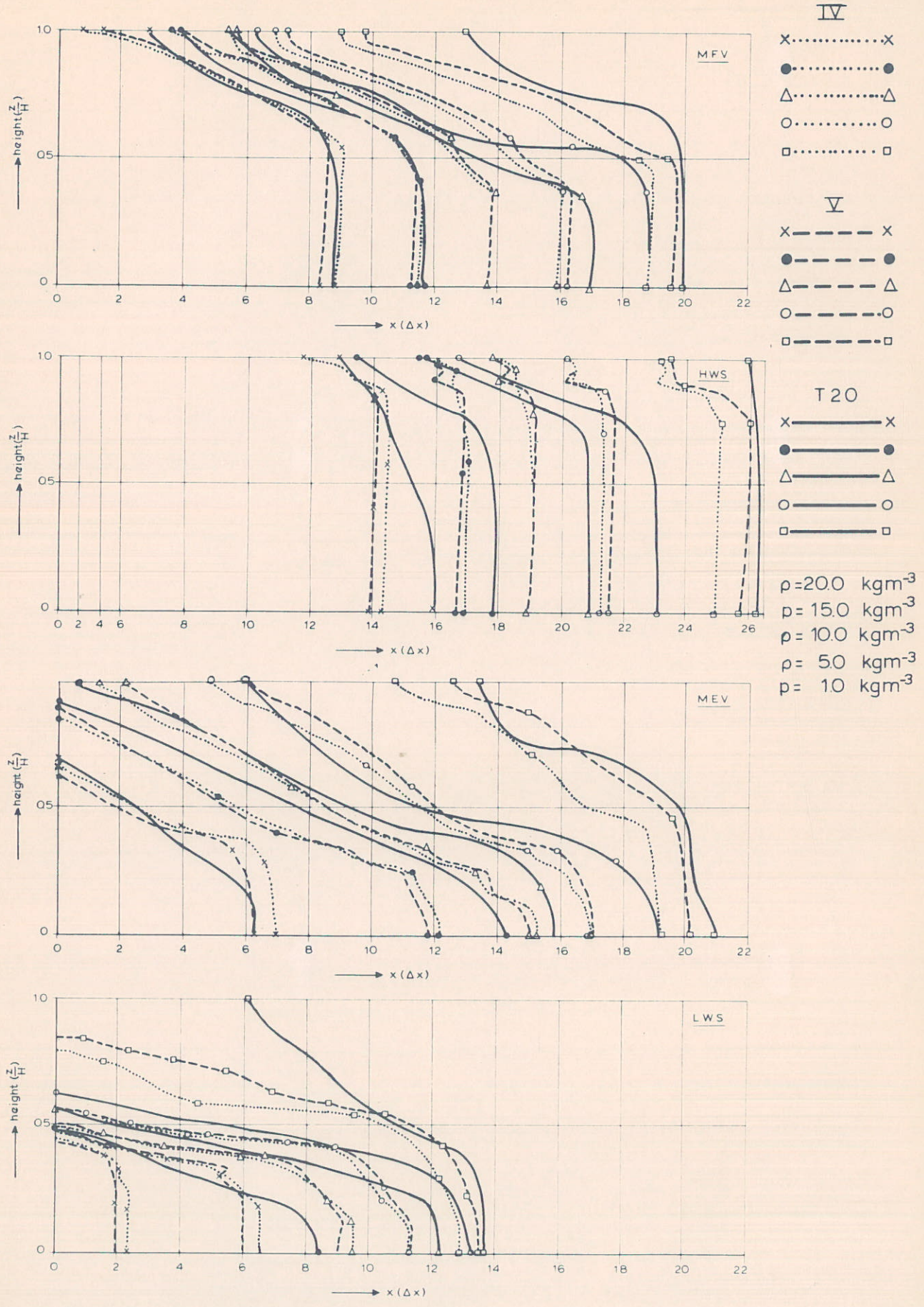

CALIBRATION WITH TIDAL FLUMEDATA
LONGITUDINAL CONCENTRATION DISTRIBUTION
AT FOUR CHARACTERISTIC TIMES

Δx=1.83 m

DELFT HYDRAULICS LABORATORY

R 897 VII

FIG. 7

CALIBRATION WITH TIDAL FLUME DATA

RELATIVE DEPTH AVERAGED CONCENTRATIONS

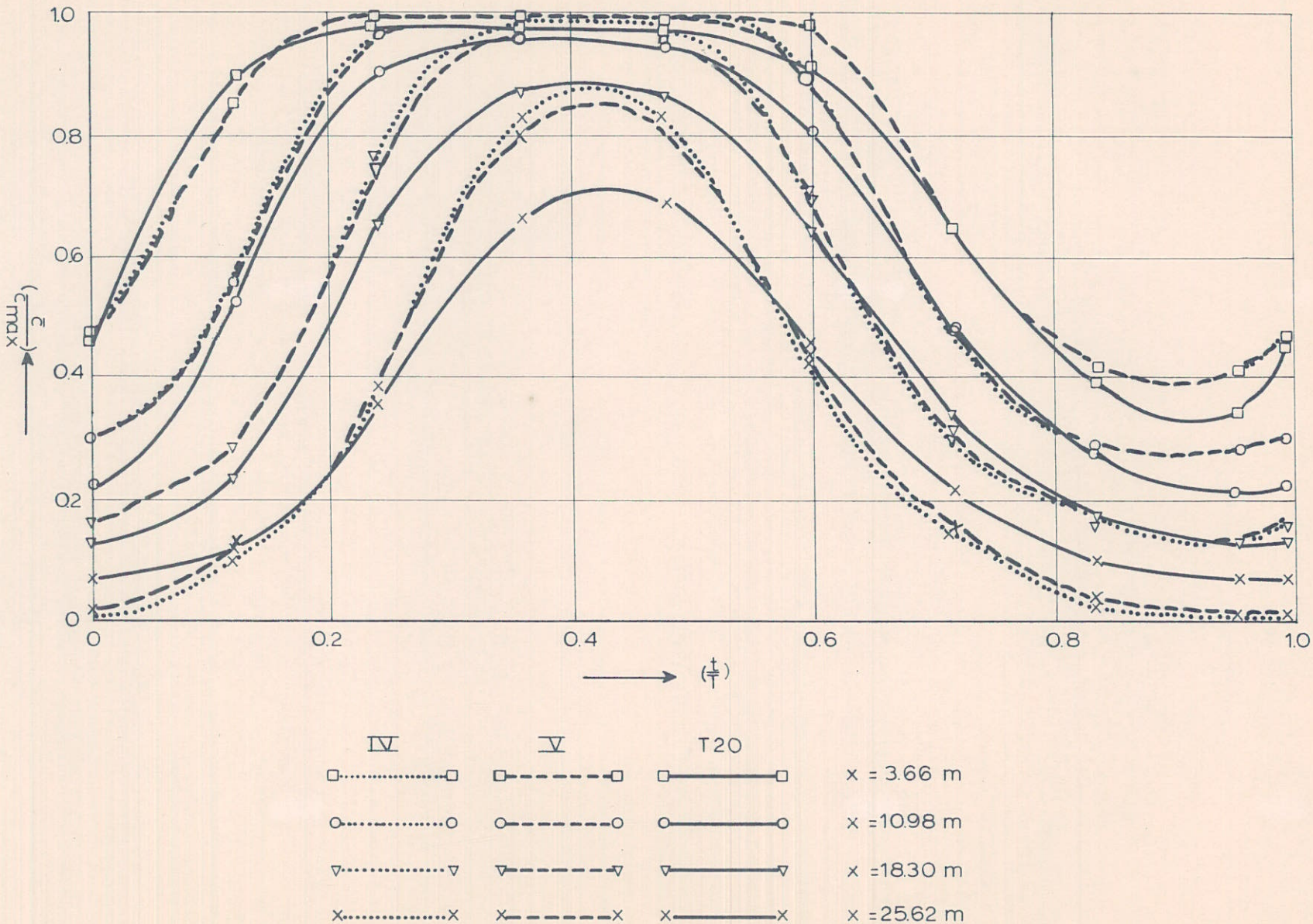

DELFT HYDRAULICS LABORATORY

R 897 VII

FIG. 8

APPENDIX I Discretisation of the boundary condition for the diffusion equation at the surface and the bottom

The diffusion equation reads:

$$\frac{\partial c}{\partial t} + \frac{\partial uc}{\partial x} + \frac{\partial wc}{\partial z} - \frac{\partial}{\partial x}\left(D_x \frac{\partial c}{\partial x}\right) - \frac{\partial}{\partial z}\left(D_z \frac{\partial c}{\partial z}\right) = 0 \qquad \text{(A1)}$$

The boundary conditions at the surface

$$D_x \frac{\partial c}{\partial x}\frac{\partial \zeta}{\partial x} - D_z \frac{\partial c}{\partial z} = 0 \qquad \text{(A2)}$$

together with the kinematic condition at the surface:

$$\frac{\partial \zeta}{\partial t} + u \frac{\partial \zeta}{\partial x} - w = 0. \qquad \text{(A3)}$$

implies that there is no transport through the surface.

When (A1) is discretised over a top layer of thickness $\Delta z/2$ with the transport through the surface taken equal to zero, the following difference equation arises:

$$\frac{c^{n+1}_{i,N_z} - c^{n}_{i,N_z}}{\tau} + \frac{(u^{n}_{i+1,N_z}\, c^{n}_{i+1,N_z} - u^{n}_{i-1,N_z}\, c^{n}_{i-1,N_z})}{2\Delta x} +$$

$$- \frac{(w^{n}_{i,N_z-1}\, c^{n+1}_{i,N_z-1} + w^{n}_{i,N_z}\, c^{n+1}_{i,N_z})}{\Delta z} +$$

$$- \left\{\frac{D_{x_{i+\frac{1}{2},N_z}} \frac{(c^{n}_{i+1,N_z} - c^{n}_{i,N_z})}{\Delta x} - D_{x_{i-\frac{1}{2},N_z}} \frac{(c^{n}_{i,N_z} - c^{n}_{i-1,N_z})}{\Delta x}}{\Delta x}\right\} +$$

$$+2\left\{\frac{D_{z_{i,N_z-\frac{1}{2}}} \frac{(c^{n+1}_{i,N_z} - c^{n+1}_{i,N_z-1})}{\Delta z}}{\Delta z}\right\} \simeq 0 \qquad \text{(A4)}$$

Analogous, a relation can be derived for the concentration at the bottom. After substitution of the boundary conditions for the momentum equation:

$$u = 0 \qquad \text{at} \qquad z = z_b \tag{A5}$$

$$w = 0 \qquad \text{at} \qquad z = z_b \tag{A6}$$

the difference equation reads:

$$\frac{c_{i,0}^{n+1} - c_{i,0}^{n}}{\tau} + \frac{(w_{i,1}^{n} \; c_{i,1}^{n+1})}{\Delta z} - \left\{ \frac{D_{x_{i+\frac{1}{2},0}} \frac{(c_{i+1,0}^{n} - c_{i,0}^{n})}{\Delta x} - D_{x_{i-\frac{1}{2},0}} \frac{(c_{i,0}^{n} - c_{i-1,0}^{n})}{\Delta x}}{\Delta x} \right\} + -2\left\{ \frac{D_{z_{i,\frac{1}{2}}} \frac{(c_{i,1}^{n+1} - c_{i,0}^{n+1})}{\Delta z}}{\Delta z} \right\} = 0 \tag{A7}$$

APPENDIX II Difference equations for the conditions of the Richardson number

The local Richardson number reads:

$$Ri = - g \frac{\frac{1}{\rho}\frac{\partial \rho}{\partial z}}{(\frac{\partial u}{\partial z})^2} . \qquad (A8)$$

For the substitution in the vertical turbulent exchange coefficients, Ri is to be discretised at level:

$$(j + \tfrac{1}{2})\Delta z. \qquad (A9)$$

in which j is an integer varying from 0 to NZ - 1.

The most simple discretisation of (A8) yields, if central differences are used:

$$Ri,j+\tfrac{1}{2} = - g \frac{(\frac{2}{\rho_{i,j+1} + \rho_{i,j}}) (\frac{\rho_{i,j+1} - \rho_{i,j}}{\Delta z})}{(\frac{u_{i,j+1} - u_{i,j}}{\Delta z})^2} \qquad (A10)$$

This discretisation was used in computation 2B and gave locally instable results: (see 4.3).

Next, an extra averaging was applied between the vertical derivatives at $z = j\Delta z$ and $z = (j+1)\Delta z$.
This gave the following discretisation of (A8):

$$Ri,j+\tfrac{1}{2} = - g \frac{(\frac{2}{\rho_{i,j+1} + \rho_{i,j}}) \tfrac{1}{2}\left[\frac{\rho_{i,j+2} - \rho_{i,j}}{2\Delta z} + \frac{\rho_{i,j+1} - \rho_{i,j-1}}{2\Delta z}\right]}{\{\tfrac{1}{2}\left[(\frac{u_{i,j+2} - u_{i,j}}{2\Delta z}) + (\frac{u_{i,j+1} - u_{i,j-1}}{2\Delta z})\right]\}^2} \qquad (A11)$$

Finally, a smoothing procedure was applied to the discretised Ri's from (A11)

$$Ri_{i,j+\frac{1}{2}} = \tfrac{1}{4} Ri_{i,j-\frac{1}{2}} + \tfrac{1}{2} Ri_{i,j+\frac{1}{2}} + \tfrac{1}{4} Ri_{i,j+1\frac{1}{2}} \qquad (A12)$$

$$Ri_{i,\frac{1}{2}} = \tfrac{3}{4} Ri_{i,\frac{1}{2}} + \tfrac{1}{4} Ri_{i,1\frac{1}{2}} \qquad (A13)$$

$$Ri_{i,N_Z-\frac{1}{2}} = \tfrac{3}{4} Ri_{i,N_Z-\frac{1}{2}} + \tfrac{1}{4} Ri_{i,N_Z-1\frac{1}{2}} \qquad (A14)$$

p.o. box 177 2600 mh delft the netherlands